Avrupa Bilim ve Teknoloji Dergisi
Özel Sayı 26, S. 16-21, Temmuz 2021

Araştırma Makalesi

www.ejosat.com ISSN:2148-2683

European Journal of Science and Technology
Special Issue 26, pp. 16-21, July 2021

Research Article

Non-Contact Micromanipulation of a Single E. *Coli* Minicell

Jiyan Sürer[1], Ahmet Fatih Tabak[2*]

[1] Kadir Has University, Faculty of Engineering and Natural Sciences, Department of Computer Engineering, Istanbul, Turkey, (ORCID: 0000-0003-3388-7843), 20181701031@stu.khas.edu.tr

[2*] Kadir Has University, Faculty of Engineering and Natural Sciences, Department of Mechatronics Engineering, Istanbul, Turkey, (ORCID: 0000-0003-3311-6942), ahmetfatih.tabak@khas.edu.tr

(3rd International Congress on Human-Computer Interaction, Optimization and Robotic Applications June 11-13, 2021)

(**DOI:** 10.31590/ejosat.944340)

ATIF/REFERENCE: Tabak, A. F. & Sürer, J. (2021). Magnetic Non-Contact Micromanipulation of a Single E. *Coli* Minicell. *European Journal of Science and Technology*, (26), 16-21.

Abstract

Today, a variety of methods are available for micro-scale transportation without inflicting damage on biological samples. There are several numerical and experimental studies in the literature that make use of microrobots to manipulate particles in non-contact performances. One of the applications used to mitigate the aforementioned risk is non-contact micro manipulation by hydrodynamic effects, and with the micro-objects floating around the core of a free vortex this method can be implemented effectively. However, a robotic model predicting the dynamics of such microsystems is rare in the literature and yet to be applied for manipulation of a bacterium. In this paper, a single magnetic particle that is assumed to be held in a fixed place while rotated by an external magnetic field, and an E. *Coli* minicell swimming in the free vortex induced by the described rotation. The mathematical model and the numerical simulations presented here via linear set of equations for rigid body-motion under the magnetic and hydrodynamic forces are built in cylindrical coordinates. Results demonstrate the numerical stability of the robotic model along with predicted-motion pointing to a steady periodic orbit around the vortex center for a total of 600 periods of simulated magnetic field rotation. Results to the numerical experiments are focused on the rigid-body rotation of E. *Coli* minicell, the propulsive force of the rotating helical tail of the bacterium, and acceleration, speed, and displacement of the bacterium with respect to the center of the vortex.

Keywords: Biomedical micro-robotics, E. *Coli* Minicell, Micromanipulation, Rigid-body motion.

Tek Bir E. *Coli* Minicell'in Temassız Mikromanipülasyonu

Öz

Biyolojik numunelerin üzerinde yapısal zarar vermeden çalışılması için günümüzde çeşitli mikro robotik yöntemler mevcuttur. Literatürde, bir mikro parçacığı çeşitli yöntemler ile manipüle etmek için mikrorobotları kullanan nümerik ve deneysel çalışmalar bulunmaktadır. Yapısal zarar görme riskini ortadan kaldıran yöntemlerden biri de hidrodinamik temassız mikro manipülasyondur. Bu yöntem, bir serbest girdap merkezi etrafında yüzen mikro parçacıkların manipülasyonuna dayanmaktadır. Ancak, halihazırda bakterilerin hidrodinamik kuvvetler yardımı ile temassız manipülasyonunu açıklamak için literatürde bir robotik model sunulmamıştır. Burada, manyetik alanlar tarafından döndürülürken sabit tutulabilen bir manyetik parçacık ve oluşan girdap akışı içerisinde yüzen bir E. *Coli* Minicell bakterisinin katı cisim davranışları çalışılmıştır. Tüm matematiksel model, silindirik koordinatlarda inşa edilmiştir. Simülasyon sonuçları, toplam 600 periyot manyetik alan dönüşü boyunca bakteri hücresi için girdap merkezi etrafında stabil ve periyodik bir yörünge öngörmüştür. Sunulan sonuçlar, bakterinin itki kuvveti ile katı cisim hareketi üzerine yoğunlaşmaktadır.

Anahtar Kelimeler: Biyomedikal mikro robotik, E. *Coli* Minicell, Mikro manipülasyon, Katı cisim hareketi.

[*] Corresponding Author: ahmetfatih.tabak@khas.edu.tr

1. Introduction

Development of biomedical micro robotic applications is an ever-growing research field (Sitti et al., 2015). It is very difficult to apply and control force in the micro world, in this particular case to manipulate cells without exerting excessive mechanical stress. However, with the development of mictotechnology and motion control, new methods have emerged. This is where rotating micro robots play an important role. Working principle of rotational microrobot is to capture and manipulate the particle by creating a vortex in the microfluidic environment. Such microrobots allow for precise sorting and characterization of micro-scale objects, such as cells, on individual level along with automatized elaborate operations (Ger et al., 2013; Paris et al., 2018; 2021). Spiral-shaped micro swimmers, i.e., bacteria-like geometries, can find the shortest path to the target with specialized algorithms such as optimum bi-directional round-trip time (Liu et al., 2020). Actuation of such micro swimmers include the utilization of reconfigurable micro-system via magnetic fields (Diller et al., 2011) and, since their environment of performance is aqueous, the overall rigid-body motion of such robots can be controoled by programming the magnetic potential energy distribution spatially and temporally (Shahrokhi et al., 2017; Dong and Sitti, 2020).

Micro-manipulation of cells can be a breakthrough in the medical field. Immersed micro-objects can be cought via the flow field of swimming micro robots to realize noncontact micromanipulation (Piat and Gauthier, 2002; Cecil et al., 2005; Khalil et al., 2020). For instance, due to angular momentum of light and its implementation in optical micromanipulation, light of certain wavelenghts can cause the trapped material to spin (Volke-Sepúlveda, 2005). Based experimental studies, optical tweezers are known to be capable of various cell manipulations (Liang et al., 2010). Additionally, due to the force balance on the volume of interest, multiple particles might tend to form spatial arrangements when captured via optical or acoustic tweezers (Nogawa et al., 2011; Gong and Baudoin, 2020) that helps manipulation and manufacturing of microrobots. However, biological samples could be damaged by heat or light (Ye and Sitti, 2014), therefore, there exist experiments in the literature showcasing the local manipulation of some bacterial species with the help of a rotating magnetic fields (Ye and Sitti, 2014). Based on the flow of moving micro vortices, it is possible to manipulate nearby particles (Petit et al., 2012). With the help of vortices created by the controlled rotation of micro robots (Peyer et al., 2011; Huang et al., 2014), particles can be gently captured and manipulated. In previous work, the free vortex flow field, caused by spinning magnetic particulate matter, is used to form curved streamlines that are modeled with the help of energy conservation and the Magnus effect indirectly applied in the equation of motion (Sürer and Tabak, 2021).

There are other methods and applications of micro manipulation. Research shows that automation of the motion of specialized microrobots is possible even with the presence of obstacles in liquid medium (Charreyron et al. 2015). Also, it was demonstrated that *Enterobacter aerogenes* can be efficiently captured and manipulated via electric field for manipulation (Mishra et al., 2016). The gait of a helical natural swimmer or microrobot can be predicted and or controlled in three dimensions based on the low Reynolds number swimming conditions (Erman and Tabak, 2014; Qiu et al., 2014; Oulmas, 2018). Finally, microrobots can be used to tow chemicals and material, although cannot strictly be classified as non-contact (Behkam and Sitti, 2006; Martel and Mohammadi, 2010; de Lanauze et al., 2013).

The main aim in this study is to capture and manipulate a bacterium instead of the normal inorganic particle. It has already been numerically shown in the literature that it is possible to interfere with the swimming trajectory of a E. *Coli* Minicell (Tabak, 2020a). In the previous study, the hydrodynamic forces exerted on a spherical particle along with the ensuing rigid-body motion was investigated (Sürer and Tabak, 2021). In this paper, the main objective is to further extend the micro robotic model and showcase its numerical stability. Therefore, the rigid-body motion of a E. *Coli* Minicell is studied while captured and forced through a circular orbit via a free vortex that is magnetically induced in an aqueous medium *in vitro*. Simulations are carried out in MATLAB environment.

2. Material and Method

The mathematical model of the previous study (Sürer and Tabak, 2021) forms the basis to consruct the equation of motion of the micro manipulation system studied here. In this particular study, there is one magnetic particle that is being held in a fixed location while being rotated via an external field and there is a single bacterium cell, E. *Coli* minicell with a spherical cell body (Chattopadhyay and Wu, 2009) that is most suitable for the modeling approach employed in this study, swimming in the vicinity of the free vortex core. Figure 1 illustrates the two aforementioned objects; the magnetic particle at the vortex center and the bacterium cell orbiting around. The bacterium cell is active and non-magnetic; thus, it experiences the propulsive force of its rotating helical tail and the drag force of the free vortex. The force balance on magnetic particle and the bacterium cell is written in cylindrical coordinates. Both particles are assumed to be neutrally buoyant and fully submersed far enough from any solid boundary for sake of simplicity (Higdon and Muldowney, 1995; Sürer and Tabak, 2021). The model, i.e., forces and rigid-body motion, presented here is constructed in the lab frame in cylindrical coordinates.

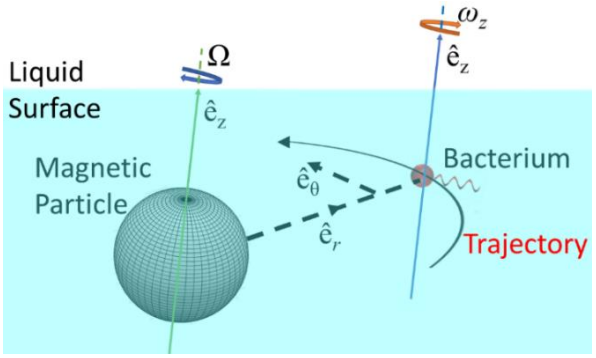

Figure 1: Magnetic particle and bacterium cell submerged in a large liquid bath. The magnetic particle being rotated by external magnetic field whereas the bacterium is trapped by the drag of the free vortex. The objects are not illustrated to scale.

The angular acceleration of the magnetic particle at the vortex core, with magnetic torque and drag torque, is given as:

$$J\frac{d\Omega}{dt} = (\boldsymbol{m} \times \Re \boldsymbol{B}) - 8\pi\mu R^3\Omega. \quad (1)$$

with **m** denoting the magnetization vector of the particle with the magnetic properties that of a N52-grade Neodymium magnet (Dong et al., 2019) along the direction of $[1\ 0\ 0]^T$. The magnetic

field, **B**, is given as $\mathbf{B} = [20\cdot\cos(2\pi\cdot f\cdot t)\ -20\cdot\cos(2\pi\cdot f\cdot t)\ 0]^{\mathrm{T}}$ mT with f = 1 Hz for the rotation rate of the field. Furthermore, J, R, and μ stand for the moment of inertia and the radius of the spherical magnetic particle, dynamic viscosity of aqueous medium, respectively. Rotation rate of the magnetic particle at the vortex core is signified by Ω. Finally, ℜ takes care of the rotation from lab frame to the inertial frame of the rotating magnetic particle.

The bacterium cell will exhibit six degrees of freedom motion when captured, three of which can simply be represented as the rigid-body translation in the lab frame whereas the rest will be rigid-body rotation in its inertial frame that is given by cylindrical coordinates (Figure 2). Furthermore, all six can be represented by a set of matrix equations. The rigid-body translation will be under the influence of the vortex-induced radial force, due to resultant pressure difference (Sürer and Tabak, 2021), the azimuthal drag of the flow field induced by the rotating magnetic particle (Sürer and Tabak, 2021) modeled based on Bernoulli equation across the streamlines (Munson et al., 2005), and the thrust force of the rotating helical tail vertically in all directions (Tabak, 2020a). Likewise, the rigid-body rotation will occur based on the shear of the free vortex and the propulsive torque of the rotating helical tail (Tabak, 2020a). It is worth mentioning that all resultant rigid-body velocities will be met with inertial and shear resistance.

Thus, the equation of motion for the bacteria is given as:

$$m\begin{bmatrix}a_r\\ a_\theta\\ a_z\end{bmatrix} = \{-6\pi\mu a u_r - \pi a^2\rho\int_{r_p-a}^{r_p+a}\frac{\left(\frac{\Omega R^2}{r}-\omega_z(r-r_p)\right)^2}{r}dr\}\hat{e}_r - 6\pi\mu a(u_\theta - v_\theta)\hat{e}_\theta + \mathbf{F}_{\mathrm{p}}, \quad (3)$$

and

$$j\begin{bmatrix}\alpha_r\\ \alpha_\theta\\ \alpha_z\end{bmatrix} = (-8\pi\mu R^2\Omega a - 8\pi\mu a^3\omega)\hat{e}_z + \mathbf{T}_{\mathrm{p}}. \quad (4)$$

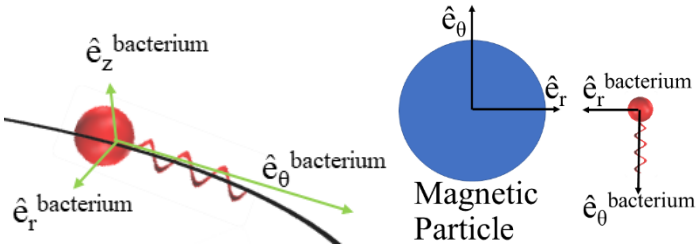

Figure 2: Depiction of the inertial frame of E. *Coli* minicell expressed in cylindrical coordinates (left); orientation of the inertial frames in the lab at t = 0 s (right).

Here, a signifies the radius of the E. *Coli* minicell as m and j stand for its mass and moment of inertia, respectively. For sake of simplicity, the moment of inertia of the rotating helical tail is omitted. Also, v_θ denotes the local azimuthal flow velocity in a proximity of r_p to the core whereas u_r and u_θ are the radial and azimuthal rigid-body velocities of the bacterium captured by the free vortex. Finally, ω_z is the integral of α_z.

The propulsive force and torque contribution of the rotating helical tail, $\mathbf{F}_{\mathrm{p}}$ and $\mathbf{T}_{\mathrm{p}}$ as given above, are modeled as (Tabak, 2020a; 2020b):

$$\begin{bmatrix}\mathbf{F}_p\\ \mathbf{T}_p\end{bmatrix} = \mathbf{M}_{tail}\begin{bmatrix}0\\0\\0\\ \omega_{tail}\\0\\0\end{bmatrix}. \quad (5)$$

Here, $\mathbf{M}_{tail}$ is the full 6×6 matrix of fluid-drag based on resistive force theory (Keller and Rubinow, 1976; Tabak, 2020a; 2020b) mapping the fluid resistance to the screw-like tail rotation, ω_{tail}, onto the main axes in the inertial frame of the E. *Coli* minicell represented in cylindrical coordinates. It is important to acknowledge that Euler angle representation (Spong et al., 2005) is summoned to find the instantaneous orientation of the bacterium cell with respect to the vortex core that is made use of to find the instantaneous position in the lab frame.

3. Results and Discussion

In this particular simulation study, the magnetic particle at the core of the free vortex is 200 μm in diameter whereas the diameter of the E. Coli *Minicell* is 0.41 μm (Chattopadhyay and Wu, 2009) and it is initially placed 110 μm away from the center of the vortex core looking in negative radial direction in the lab frame as depicted in Figure 2 (right). Simulation results not only demonstrate the dynamics of the manipulated bacterium but also the stability of the mathematical model presented here via a long run for a total of 600 seconds in real-time. The rigid-body motion is studied along the rθ-plane for neutrally buoyant particle and bacterium. All results are obtained with the help of MATLAB 2020a and presented in the lab frame, i.e. $[\hat{e}_r\ \hat{e}_\theta\ \hat{e}_z]^{\mathrm{T}}$.

Figure 3 demonstrates the radial and azimuthal propulsive force components induced by the rotating helical tail of the bacterium cell. Extrema of both components are in the order of O(–13) and oscillate around zero. Also, Figure 4 gives the radial pressure force exerted on the body of the bacterium, which is predicted by Bernoulli's equations (Sürer and Tabak, 2021; Munson et al., 2005) on the radial direction, and the azimuthal drag force of the free vortex acting, again, on the body of the bacterium. The pressure force is oscillating with an apparent negative mean, as expected, and in the order of O(–19). On the other hand, the azimuthal drag on the bacterium is oscillating with a negative mean on the order of O(–13) thus overcoming the propulsive force as will be evident.

Figure 5 represents a comparison of the said force components over 10 seconds in real-time. The rotation rate of E. *Coli* Minicell is 78 Hz (Chattopadhyay and Wu, 2009). Furthermore, the bacterium exhibits complex rigid-body rotations (Tabak, 2018). As a result, components of the propulsive force are found to be highly nonlinear. On the other hand, the main component of the oscillation in drag and pressure forces of the free vortex due to step-out phenomenon (Sürer and Tabak, 2021), as visualized in Figure 5. Finally, the higher order component in the rigid-body z-rotation of the bacterium happens to be the combined result of the shear of the azimuthal stream and the propulsive torque on the body.

Figure 6 depicts the radial acceleration, velocity, and displacement of the bacterium with respect to the vortex core. The rigid-body displacement exhibits an oscillatory behavior with the order of O(–5); therefore, arguably following a stable orbit around the rotating magnetic particle. Although the instantaneous radial velocity is observed to be higher than one

body length per unit time; however, the radial proximity is found to be almost steady periodic.

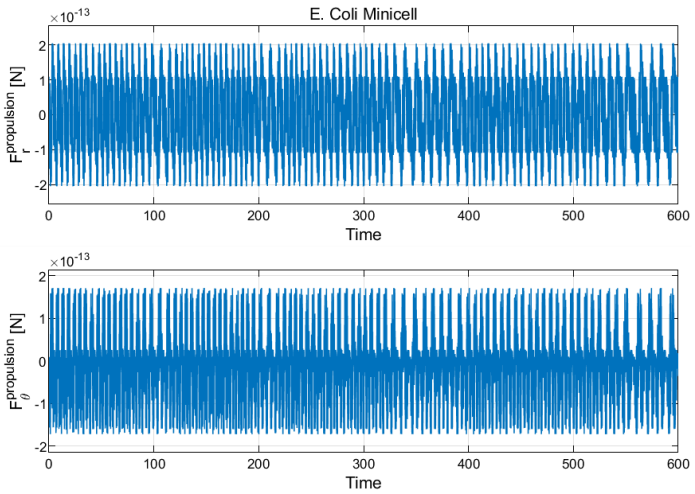

Figure 3: Propulsive force of the rotating helical tail along radial (top) and azimuthal (bottom) directions.

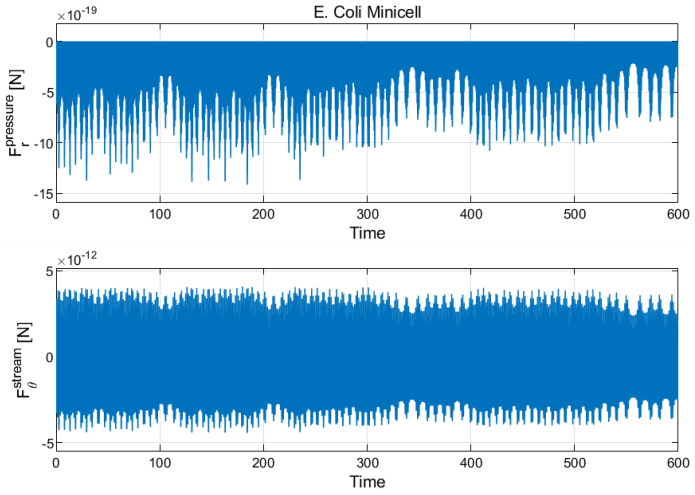

Figure 4: Radial (pressure, top) and azimuthal (stream, bottom) force of the free vortex on the E. *Coli* minicell.

Figure 7 demonstrates the rigid-body motion of bacterium in the azimuthal direction around the vortex core. The net displacement in 600 seconds is on the order of $O(-1)$, thus the model predicts that the bacterium is coerced to orbit the vortex core several times per unit time. In the meantime, the azimuthal velocity oscillates with the order of $O(-4)$.

Figure 8 demonstrates the total rigid-body rotation of the magnetic particle at the vortex core and the total rigid-body rotation of the bacterium around the vortex core in lab frame. It can be observed that the bacterium orbits the magnetic vortex core ~130 times while the magnetic core itself completes ~160 full rotations over a time-span of 600 seconds.

Figure 9 demonstrates the lateral rigid-body rotation behavior of the bacterium in its inertial frame. The rotation rate along z-axis is affected by the shear exerted on the bacterium body by the free vortex. On the other hand, the rotation along r-axis is dominated only by the propulsive torque and opposing fluid resistance. Furthermore, the radial rotation is omissible in comparison to the z-rotation.

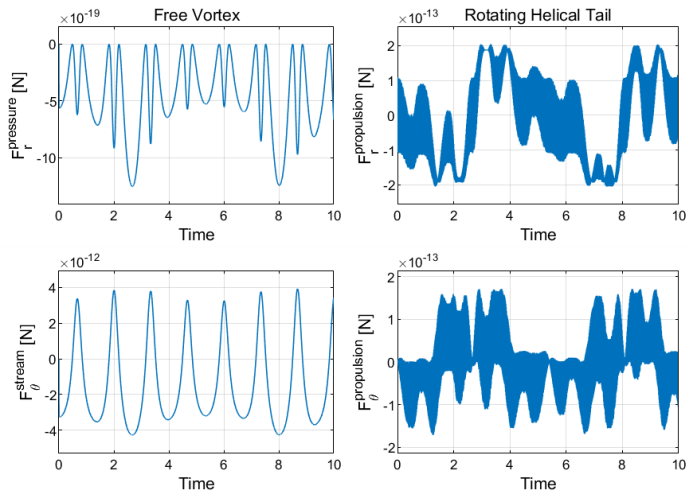

Figure 5: Comparison of force components acting on the E. *Coli* Minicell with (a) induced by free vortex (left-hand-side) and induced by rotating helical tail (right-hand-side); (b) pressure and propulsive forces acting along the radial direction (top) and drag and propulsive forces acting along the azimuthal direction (bottom).

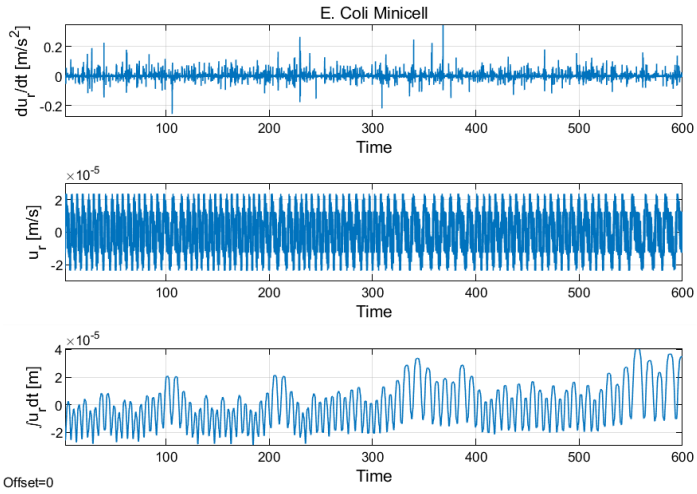

Figure 6: Radial acceleration (top), velocity (middle), and displacement (bottom) of the E. *Coli* minicell trapped by the free vortex.

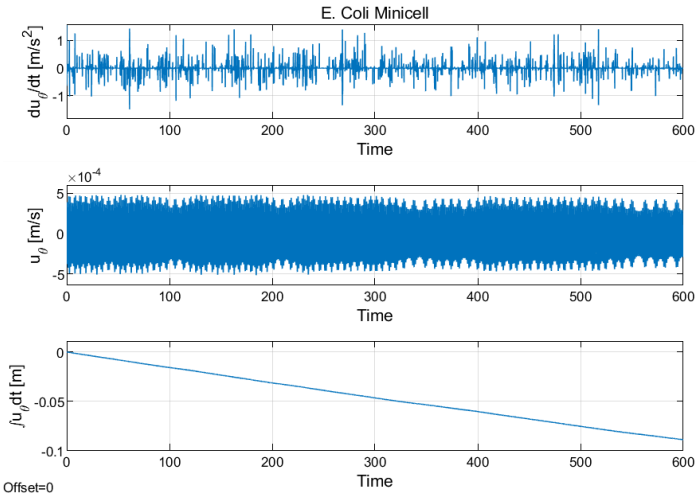

Figure 7: Azimuthal acceleration (top), velocity (middle), and displacement (bottom) of the E. *Coli* minicell trapped by the free vortex.

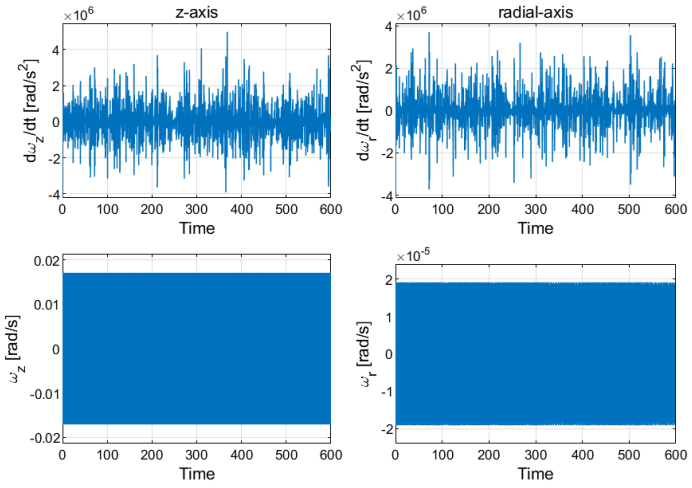

Figure 8: Lateral rigid-body rotation, acceleration (top) and velocity (left), of E. *Coli* minicell in inertial frame of the bacterium; along z-axis (left-hand-side) and along radial-axis (right-hand-side).

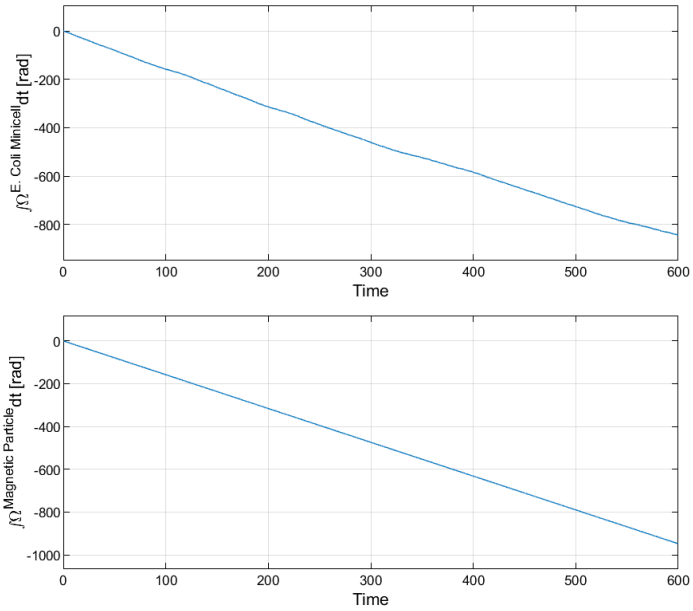

Figure 9: The total rotation of the E. *Coli* minicell around the vortex core (top) and the total rotation of the magnetic particle at the vortex core (bottom).

4. Conclusions and Recommendations

The robotic model is demonstrated to be numerically stable and the simulations predicted a steady periodic orbit around the vortex core for about 600 period of magnetic field rotation. Therefore, it is arguably possible to manipulate the motion of a live bacteria although we did not include random walks in the simulation. Thus, Brownian noise should be included in the model to study the effect of stochastic rigid-body motion. In the meantime, given that the results are presented for Newtonian flow conditions, the model should further be improved to include non-Newtonian fluids to ascertain how shear-thinning phenomenon would affect the stability of the orbit. Furthermore, the E. *Coli* Minicell did not collide with the magnetic particle avoiding the danger of getting stuck on its surface due to electrostatic effects that are not included in the model.

Addressable manipulation of a bacterium will only be possible if multiple rotating cores are employed in tandem so the superimposed effect of adjacent free vortices could be harnessed to coerce the cell to move along a relatively straight path. A matrix of rotating cores will make it possible to sort multiple bacteria based on their body size and shape owing to distinct shear drag they would experience. However, this brings out the problem of controlling multiple magnetic cores simultaneously that might dictate the requirement of a specifically tailored magnetic field and actuation system dynamics for the desired application.

References

[1] Liu, J., Wu, X., Huang, C., Manamanchaiyaporn, L., Shang, W., Yan, X., & Xu, T. (2020). 3-D Autonomous Manipulation System of Helical Microswimmers With Online Compensation Update. IEEE Transactions on Automation Science and Engineering.

[2] Oulmas, A., Andreff, N., & Régnier, S. (2018). 3D closed-loop swimming at low Reynolds numbers. The International Journal of Robotics Research, 37(11), 1359-1375.

[3] Cecil, J., Vasquez, D., & Powell, D. (2005). A review of gripping and manipulation techniques for micro-assembly applications. International Journal of Production Research, 43(4), 819-828.

[4] Piat, E., & Gauthier, M. (2002). An electromagnetic micromanipulation system for single-cell manipulation. Journal of Micromechatronics, 2(2), 87-119.

[5] Diller, E., Pawashe, C., Floyd, S., & Sitti, M. (2011). Assembly and disassembly of magnetic mobile micro-robots towards deterministic 2-D reconfigurable micro-systems. The International Journal of Robotics Research, 30(14), 1667-1680.

[6] Sitti, M., Ceylan, H., Hu, W., Giltinan, J., Turan, M., Yim, S., & Diller, E. (2015). Biomedical applications of untethered mobile milli/microrobots. Proceedings of the IEEE, 103(2), 205-224.

[7] Liang, Y. L., Huang, Y. P., Lu, Y. S., Hou, M. T., & Yeh, J. A. (2010). Cell rotation using optoelectronic tweezers. Biomicrofluidics, 4(4), 043003.

[8] Khalil, I. S., Klingner, A., Hamed, Y., Hassan, Y. S., & Misra, S. (2020). Controlled Noncontact Manipulation of Nonmagnetic Untethered Microbeads Orbiting Two-Tailed Soft Microrobot. IEEE Transactions on Robotics, 36(4), 1320-1332.

[9] Dong, X., & Sitti, M. (2020). Controlling two-dimensional collective formation and cooperative behavior of magnetic microrobot swarms. The International Journal of Robotics Research, 39(5), 617-638.

[10] Ye, Z., & Sitti, M. (2014). Dynamic trapping and two-dimensional transport of swimming microorganisms using a rotating magnetic microrobot. Lab on a Chip, 14(13), 2177-2182.

[11] Huang, T. Y., Qiu, F., Tung, H. W., Chen, X. B., Nelson, B. J., & Sakar, M. S. (2014). Generating mobile fluidic traps for selective three-dimensional transport of microobjects. Applied Physics Letters, 105(11), 114102.

[12] Nogawa, K., Kojima, M., Nakajima, M., Homma, M., Arai, F., & Fukuda, T. (2011, November).

Improvement of motility of bacterium-driven microobject fabricated by optical tweezers. In 2011 International Symposium on Micro-NanoMechatronics and Human Science (pp. 482-485). IEEE.

[13] Peyer, K. E., Zhang, L., & Nelson, B. J. (2011). Localized non-contact manipulation using artificial bacterial flagella. Applied Physics Letters, 99(17), 174101.

[14] Ger, T. R., Huang, H. T., Chen, W. Y., & Lai, M. F. (2013). Magnetically-controllable zigzag structures as cell microgripper. Lab on a Chip, 13(12), 2364-2369.

[15] Charreyron, S., Pieters, R. S., Tung, H. W., Gonzenbach, M., & Nelson, B. J. (2015, September). Navigation of a rolling microrobot in cluttered environments for automated crystal harvesting. In 2015 IEEE/RSJ International Conference on Intelligent Robots and Systems (IROS) (pp. 177-182). IEEE.

[16] Paris, A., Decanini, D., & Hwang, G. (2018). On-chip multimodal vortex trap micro-manipulator with multistage bi-helical micro-swimmer. Sensors and Actuators A: Physical, 276, 118-124.

[17] Petit, T., Zhang, L., Peyer, K. E., Kratochvil, B. E., & Nelson, B. J. (2012). Selective trapping and manipulation of microscale objects using mobile microvortices. Nano letters, 12(1), 156-160.

[18] Shahrokhi, S., Lin, L., Ertel, C., Wan, M., & Becker, A. T. (2017). Steering a Particle Swarm Using Global Inputs and Swarm Statistics. arXiv preprint arXiv:1706.02162.

[19] Qiu, T., Lee, T. C., Mark, A. G., Morozov, K. I., Münster, R., Mierka, O., Turek, S., Leshansky, M., A., & Fischer, P. (2014). Swimming by reciprocal motion at low Reynolds number. Nature communications, 5(1), 1-8.

[20] Paris, A., Decanini, D., & Hwang, G. (2021). Swimming force characterizations of multistaged bi-helical microswimmer and 3D vortex trap manipulation. Microelectronic Engineering, 235, 111466.

[21] de Lanauze, D., Felfoul, O., Turcot, J. P., Mohammadi, M., & Martel, S. (2013). Three-dimensional remote aggregation and steering of magnetotactic bacteria microrobots for drug delivery applications. The International Journal of Robotics Research, 33(3), 359-374.

[22] Gong, Z., & Baudoin, M. (2020). Three-dimensional trapping and assembly of small particles with synchronized spherical acoustical vortices. Physical Review Applied, 14(6), 064002.

[23] Behkam, B., & Sitti, M. (2006, August). Towards hybrid swimming microrobots: bacteria assisted propulsion of polystyrene beads. In 2006 International Conference of the IEEE Engineering in Medicine and Biology Society (pp. 2421-2424). IEEE.

[24] Mishra, A., Maltais, T. R., Walter, T. M., Wei, A., Williams, S. J., & Wereley, S. T. (2016). Trapping and viability of swimming bacteria in an optoelectric trap. Lab on a Chip, 16(6), 1039-1046.

[25] Martel, S., & Mohammadi, M. (2010, May). Using a swarm of self-propelled natural microrobots in the form of flagellated bacteria to perform complex micro-assembly tasks. In 2010 IEEE International Conference on Robotics and Automation (pp. 500-505). IEEE.

[26] Volke-Sepúlveda, K. (2005, April). Vortex Beams and Modern Techniques in Optical Micromanipulation. In AIP Conference Proceedings (Vol. 759, No. 1, pp. 43-51). American Institute of Physics.

[27] Sürer, J., & Tabak, A. F. (2021). Bernoulli-Equation-Based Robotic Model for Non-Contact Magnetic Micromanipulation. European Journal of Science and Technology, (24), 47-52. https://doi.org/10.31590/ejosat.899657

[28] Chattopadhyay, S., & Wu, X. L. (2009). The Effect of Long-Range Hydrodynamic Interaction on the Swimming of a Single Bacterium. Biophysical Journal, 96(5), 2023–2028. https://doi.org/10.1016/j.bpj.2008.11.046

[29] Higdon, J. J. L., & Muldowney, G. P. (1995). Resistance functions for spherical particles, droplets and bubbles in cylindrical tubes. *Journal of Fluid Mechanics*, *298*, 193–210. https://doi.org/10.1017/s0022112095003272

[30] Dong, F., Huang, Z., Qiu, D., Hao, L., Wu, W., & Jin, Z. (2019). Design and Analysis of a Small-Scale Linear Propulsion System for Maglev Applications (1)—The Overall Design Process. *IEEE Transactions on Applied Superconductivity*, *29*(2), 1–5. https://doi.org/10.1109/tasc.2019.28953

[31] Munson, B. R., Young, D. F., & Okiishi, T. H. (2005). *Fundamentals of Fluid Mechanics* (5th ed.). Wiley.

[32] Tabak, A. F. (2020a, June). Adaptive Motion Control of Modified E. Coli. 2020 *International Congress on Human-Computer Interaction, Optimization and Robotic Applications (HORA)*. https://doi.org/10.1109/hora49412.2020.9152603

[33] Tabak, A. F. (2020b). Bilateral control simulations for a pair of magnetically-coupled robotic arm and bacterium for in vivo applications. *Journal of Micro-Bio Robotics*, *16*(2), 199–214. https://doi.org/10.1007/s12213-020-00138-z

[34] Keller, J., & Rubinow, S. (1976). Swimming of flagellated microorganisms. *Biophysical Journal*, *16*(2), 151–170. https://doi.org/10.1016/s0006-3495(76)85672-x

[35] Spong, M. W., Hutchinson, S., & Vidyasagar, M. (2005). *Robot Modeling and Control* (1st ed.). Wiley.

[36] Erman, A. G., & Tabak, A. F. (2014, July). Resistive force theory based modeling and simulation of surface contact for swimming helical micro robots with channel flow. 2014 IEEE/ASME International Conference on Advanced Intelligent Mechatronics. https://doi.org/10.1109/aim.2014.6878110